

Structural and Functional Optical Imaging of Three-Dimensional Engineered Tissue Development

WEI TAN, Ph.D.,¹ AYLIN SENDEMIR-URKMEZ, M.S.,² LESTER J. FAHRNER, B.S.,³
RUSSELL JAMISON, Ph.D.,^{1,3,4} DEBORAH LECKBAND, Ph.D.,^{1,4,5}
and STEPHEN A. BOPPART, M.D., Ph.D.^{1,3,4,6}

ABSTRACT

A significant amount of the data collected by cell biologists and tissue engineers relies on invasive imaging techniques to visualize dynamic structural and functional properties in engineered tissues. We report the use of optical coherence tomography and the comparative use of confocal microscopy to nondestructively and noninvasively monitor the structural and functional characteristics of three-dimensional engineered tissues over time. The engineered tissue model is composed of chitosan scaffolds and fibroblasts transfected with vinculin fused to green fluorescent protein. We image the developmental process of engineered tissues from changes of tissue microarchitecture to cell–matrix adhesions in three dimensions. These findings demonstrate the potential for optical coherence tomography in applications in cell and tissue biology, tissue engineering, and drug discovery.

INTRODUCTION

CELL ACTIVITIES in three-dimensional (3-D) engineered tissues are of great interest for both basic cell biology research and applications, such as tissue engineering and pharmacological research.^{1,2} Invasive imaging methods such as histology and scanning electron microscopy (SEM) are used predominantly to evaluate the development process of engineered tissues and cellular responses to environmental stimuli. These invasive methods, however, have intrinsic disadvantages. These methods do not permit real-time or dynamic imaging, lack real 3-D information, require long and harsh processing steps at discrete time points, and make structure–function correlations difficult. Consequently, despite a tremendous increase in tissue-engineering research, few have investigated the dynamics of cell behaviors and biological interactions in engineered tissues. The primary limitation

has been inadequate imaging technology for high-resolution, real-time, noninvasive imaging deep within highly scattering tissues.

Confocal microscopy (CM) has been an important advance in microscopy and has enabled the imaging of intact, optically nontransparent specimens to produce high-resolution (submicron) images of tissue structure with the use of fluorescent probes.^{3–5} For a relatively thick specimen (up to several hundred microns), CM accomplishes optical sectioning by scanning the specimen with a focused beam of light and collecting the fluorescence signal via a pinhole aperture that spatially rejects light from out-of-focus areas of the specimen. Imaging depths, however, are limited to a few hundred microns and exogenous fluorescence probes are usually required for detection, often limiting the long-term viability of the cells being imaged. Confocal microscopy can be performed in reflectance mode, without the use of fluorescent probes,

¹Beckman Institute for Advanced Science and Technology, ²Department of Materials Science and Engineering, ³Department of Electrical and Computer Engineering, ⁴Department of Bioengineering, ⁵Department of Chemical and Biomolecular Engineering, and ⁶College of Medicine, University of Illinois at Urbana-Champaign, Urbana, Illinois.

to provide detailed images of tissue architecture and cellular morphology of living tissue in near real-time.⁶⁻⁸ This method of confocal imaging with reflected light relies on the differential backscattering properties from cellular morphology and tissue architecture to provide contrast. Hence, it resembles histological tissue evaluation, except that the subcellular resolution is achieved noninvasively and without stains. Although promising for real-time longitudinal studies, it still has penetration limitations, particularly for highly scattering tissues.

Multiphoton microscopy, which relies on the simultaneous absorption of two or more near-infrared photons from a high-intensity short-pulse laser (most commonly a mode-locked titanium:sapphire laser) extends the imaging depth of CM, but still with depth limitations of about 400–500 μm .^{9,10} Longer wavelength excitation light in multiphoton microscopy has the additional advantages of being scattered and absorbed less in biological tissue, resulting in improved imaging depths with little thermal damage. Newer technologies for imaging engineered tissues, including high-field strength magnetic resonance imaging and microcomputed tomography, have been pursued for the assessment of cellular structure, with limited success. These techniques, with long data acquisition rates, hazards associated with high-energy radiation, and relatively high costs, are less suitable for both real-time and long-term imaging.^{11,12}

Optical coherence tomography (OCT) is an emerging technique that has the potential for overcoming many of the limitations of the current technologies.^{13,14} OCT measures the intensity of backreflected near-infrared light. OCT combines the high resolutions of most optical techniques with an ability to reject multiply scattered photons and, hence, image at cellular resolutions (several microns) up to several millimeters deep in nontransparent (highly scattering) tissue. Because OCT relies on variations in indices of refraction and optical scattering for image contrast, no exogenous fluorophores are necessary, enabling cellular imaging within living specimens over time without loss of viability. Near-infrared light is scattered less than visible light. Therefore, the use of near-infrared wavelengths in OCT enables deep imaging penetration within highly scattering tissues. OCT has been applied *in vivo* for imaging the microstructures of different tissues including the eye, skin, gastrointestinal tract, and nervous systems, to name only a few, and is becoming a promising and powerful imaging technology that has widespread applications throughout many fields of biology and medicine.¹⁵⁻²⁰ However, for dynamically evaluating engineered tissues, the optical properties of these constructs are not as obvious or well characterized as for *in vivo* tissues. Few studies have investigated the use of the OCT technology for monitoring developing *in vitro*-engineered tissues.^{21,22}

In this article, we report the use of OCT as a noninvasive imaging modality to explore 3-D microstructures

and cell activities during the growth of engineered tissues. OCT is capable of clearly identifying tissue microstructures and cell distributions, determining the stages of tissue development at a level of detail approaching conventional histology, and generating 3-D images of tissue morphology. Compared with other microscopy imaging approaches, OCT permits high-resolution, real-time, deep-tissue, 3-D imaging to be performed rapidly and repeatedly over extended periods of time with intact, living specimens. Furthermore, imaging of engineered tissues with both OCT and CM demonstrates their synergistic applications for 3-D dynamic structural and functional visualizations. This powerful approach to the noninvasive imaging of the morphology and function of engineered tissues has enormous potential for a wide range of applications ranging from tissue engineering to drug discovery.

MATERIALS AND METHODS

Cell preparation

Engineered tissues are composed of cells, extracellular matrices, and 3-D scaffolds. In our study, NIH 3T3 cells (American Type Culture Collection [ATCC], Manassas, VA) seeded in a porous chitosan scaffold were used as an engineered tissue model. Cells were transfected with a green fluorescent protein (GFP)–vinculin plasmid, forming a stable cell line that expressed GFP–vinculin. For transfection, 7×10^5 cells were seeded on each well of a 6-well plate. For each well of cells, 4 μg of DNA and 2 μL of Lipofectamine 2000 reagent were diluted separately with 50 μL of FreeStyle 293 expression medium and then mixed and cultured for 20 min to form DNA–LF2000 complexes. The concentration of cells and DNA was determined in pilot experiments to be optimal for transfection efficiency.

Cell culture

Cell cultures were maintained in an incubator at 37°C and with 5% CO₂. For real-time imaging, cell culture was performed in a portable microincubator (LU-CPC, Harvard Apparatus, Holliston, MA) that was placed on the microscope stages for imaging.

Scaffold preparation

Chitosan scaffolds were prepared according to the following procedure: 2% (wt%) chitosan flakes (Sigma, St. Louis, MO) were dissolved in a 0.2 M acetic acid aqueous solvent. The resulting viscous solution was filtered and transferred to cylindrical molds. Cylinders were frozen at a rate of 0.3°C/min from room temperature to –20°C. Frozen cylinders (8 mm in diameter and 3 mm in height) were lyophilized for 4 days for complete re-

removal of the solvent. The resulting sponges had an interconnected porosity of $>80\%$ with an average pore size of $100\ \mu\text{m}$. Scaffolds were sterilized with 80% ethanol and then rehydrated through a series of ethanol/phosphate-buffered saline (PBS) solutions (70, 50, and 0% ethanol), and finally transferred to the final culture medium for overnight hydration. Seeding was done by plating $50\ \mu\text{L}$ of a concentrated cell suspension on the scaffolds at a seeding density of 5×10^6 cells/cm³.

Optical coherence tomography

OCT imaging was performed on engineered tissues after 1, 3, and 7 days of culture. Our fiber-based OCT system used a Nd:YVO₄-pumped titanium:sapphire laser as a broad-bandwidth optical source that produced 500 mW of average power and approximately 90-fs pulses with an 80-MHz repetition rate at an 800-nm center wavelength. Laser output was coupled into an ultrahigh numerical aperture fiber (UHNA4; Thorlabs, Karlsruhe, Germany) to spectrally broaden the light from 20 nm to more than 100 nm, improving the axial resolution of our system from 14 to 3 μm . The reference arm of the OCT interferometer con-

tained a galvanometer-driven retroreflector delay line that was scanned a distance of 2 mm at a rate of 30 Hz. The sample arm beam was focused into the tissue by an achromatic lens (12.5 mm in diameter, 20 mm in focal length) to a 10- μm -diameter spot size (transverse resolution). The 12-mW beam was scanned over the engineered tissue with a galvanometer-controlled mirror. The envelope of the interference signal was digitized to 12-bit accuracy.

Confocal microscopy imaging

Confocal scanning microscopy (LCSM) (model DM-IRE; Leica Microsystems, Bensheim, Germany) was used to acquire stacks of 3-D fluorescent images. An argon laser line at a wavelength of 488 nm was used to excite the GFP and autofluorescent signal, and the 514-nm wavelength was detected as the reflection signal. Samples were imaged in the sequential scanning mode with $\times 20$ and $\times 40$ objectives. The autofluorescence of chitosan was detected in the same detection channel as the GFP emission. A dye separation algorithm provided by Leica Microsystems was used to separate the fluorescence signals.

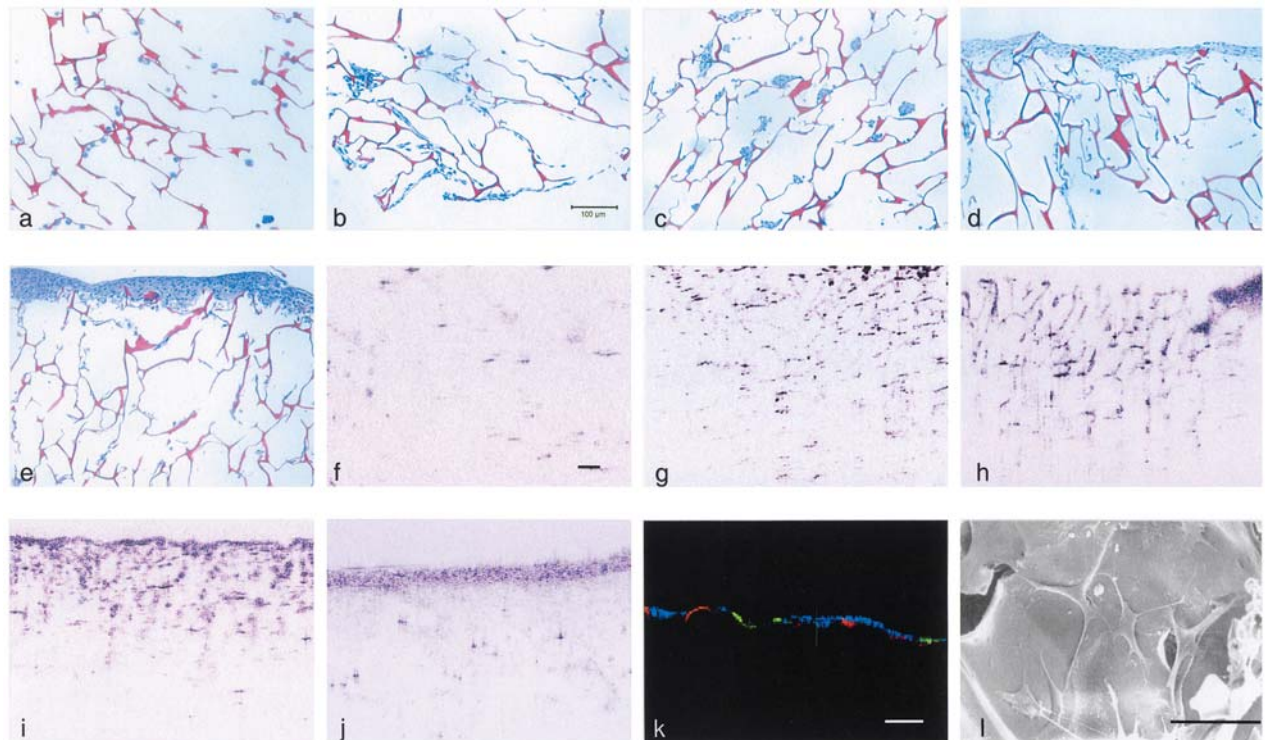


FIG. 1. x - z cross-sectional images from histology (**a-e**), OCT (**f-j**), confocal microscopy (**k**), and scanning electron microscopy (**l**). Engineered tissues with cells seeded in 100- μm pore size chitosan scaffolds were cultured for different time periods: 1 day (**a** and **f**), 3 days (**b** and **g**), 5 days (**c** and **h**), 7 days (**d** and **i**), and 9 days (**e** and **j**). Confocal microscopy (**k**) and SEM (**l**) are shown for the engineered tissues cultured for 3 days. The scale bars shown in (**b**) [for (**a-e**)], (**f**) [for (**f-j**)], and (**k**) all represent 100 μm . The scale bar in (**l**) represents 50 μm . In histological images (**a-e**), the chitosan scaffold is shown stained red, the cells are dark purple, and the matrices are light purple.

Histology

Samples were fixed in 3.7% formaldehyde, embedded in paraffin, cut into 5- μm ultrathin sections with a microtome, and stained with hematoxylin and eosin for light microscopy observations.

Scanning electron microscopy

Engineered tissues were fixed with 2.5% glutaraldehyde in a 0.1 M cacodylate buffer (pH 7.4) for 1 h at room temperature and then submerged in 1 wt% osmium tetroxide in 0.1 M sodium cacodylate for 1.5 h. The specimens were washed with 0.1 M cacodylate buffer before dehydration through a series of graded alcohol solutions. Specimens were placed in hexamethyldisilazane (HMDS; Electron Microscopy Sciences, Fort Washington, PA) for drying for 45 min before drawing it off. Samples were dried under a fume hood at room temperature and then transferred to a dry well. The resulting samples were sputter coated and examined with a scanning electron microscope.

Three-dimensional reconstruction

Three-dimensional images were reconstructed with Slicer Dicer (Pixotec, Renton, WA) and Analyze 5.0 (Mayo Clinic, Rochester, MN).

RESULTS AND DISCUSSION

Comparison of imaging tools

OCT and CM were used to noninvasively examine the growth of engineered tissues. For real-time observation, living tissue samples were loaded into a sterile microincubator that was subsequently placed onto the stages of these microscopes. Conventional histology and SEM were performed on the same specimens to correlate structural observations between modalities. The use of these latter two modalities, however, required that samples be fixed, sectioned, and stained according to standard procedures.

The representative engineered tissue model for these studies is composed of a chitosan scaffold (pore size, 100 μm) and fibroblasts transfected with vinculin fused to green fluorescent protein (GFP). Vinculin is an abundant cytoskeletal protein found in integrin-mediated focal adhesions and also in cadherin-mediated cell–cell adherens junctions. Vinculin expression therefore reflects the degree of cell–cell and cell–substrate adhesions. Figure 1 compares x – z cross-sectional images obtained by OCT, histology, and CM. From both the histology and OCT images, several stages of engineered tissue development can be clearly identified. In the initial stage (0–1 day after cell seeding) cells began attaching to the scaffold, and

are mostly spherical in appearance (Fig. 1a). During the next 2–4 days, cells displayed an elongated morphology and deposited matrices (Fig. 1b and c). After several more days, cells lost viability deep within the tissue, or migrated to the surface, forming a thick superficial layer of cells (Fig. 1d and e).

The OCT images demonstrate similar trends in the structural properties of engineered tissue during development, as in the histological images. The chitosan scaffold alone, without adherent cells, was not visible by OCT. This is attributed to the thin cross-sectional dimension (typically less than 5 μm) of the scaffold wall, and the low backscattering optical property of the material. However, after cells were seeded and cultured in the scaffold, the microstructure of the engineered tissues became visible by OCT. Figure 1f shows initial cell attachment. Cells initially appear as small highly backscattering regions in the image. Cells and extracellular matrices are readily apparent compared with the low backscattering chitosan scaffold. Figure 1g and h shows that cells are uniformly distributed throughout the chitosan scaffold after 3–5 days in culture (high cell viability deep within the tissue), and that the cell number and matrix density increase with culture time. Figure 1i and j shows an uneven distribution in the engineered tissues after 7–9 days in culture. Cells and matrices are dense in the first 100–200 μm , forming a more highly scattering layer near the tissue surface. Cells and deposited matrices are less abundant deep within the scaffold. Compared with the CM cross-sectional image obtained from a reconstructed 3-D data set (Fig. 1k), OCT image penetration is significantly deeper (2 mm versus 150 μm), and is close to the observation depth of the histological images and the size of these scaffolds. Thus, OCT clearly extracts critical structural information during the development of engineered tissues. However, because of the small size of the differentiated cells, the individual cell morphology cannot be imaged at the current OCT imaging resolution.

With lower imaging penetration but high resolution, confocal images demonstrated similar structural changes of tissue components at various stages, as well as changes in cell morphology and matrices in the near-surface layer (100–200 μm) (Fig. 2). All of the CM images in Fig. 2 are 3-D data sets projected onto the x – y plane. In the three-color images, red shows the autofluorescence signal from the chitosan scaffolds, green shows the GFP–vinculin expressed by cells, and blue shows the reflection signal from the tissue, mostly from the matrices in the tissue, but also with some contribution from highly reflective regions of the chitosan scaffold and from nonviable cells. In the initial culture stage (Fig. 2a), little secreted matrix exists in the scaffold (the bright blue regions here are likely highly reflecting surfaces of chitosan), and the vinculin is expressed uniformly over

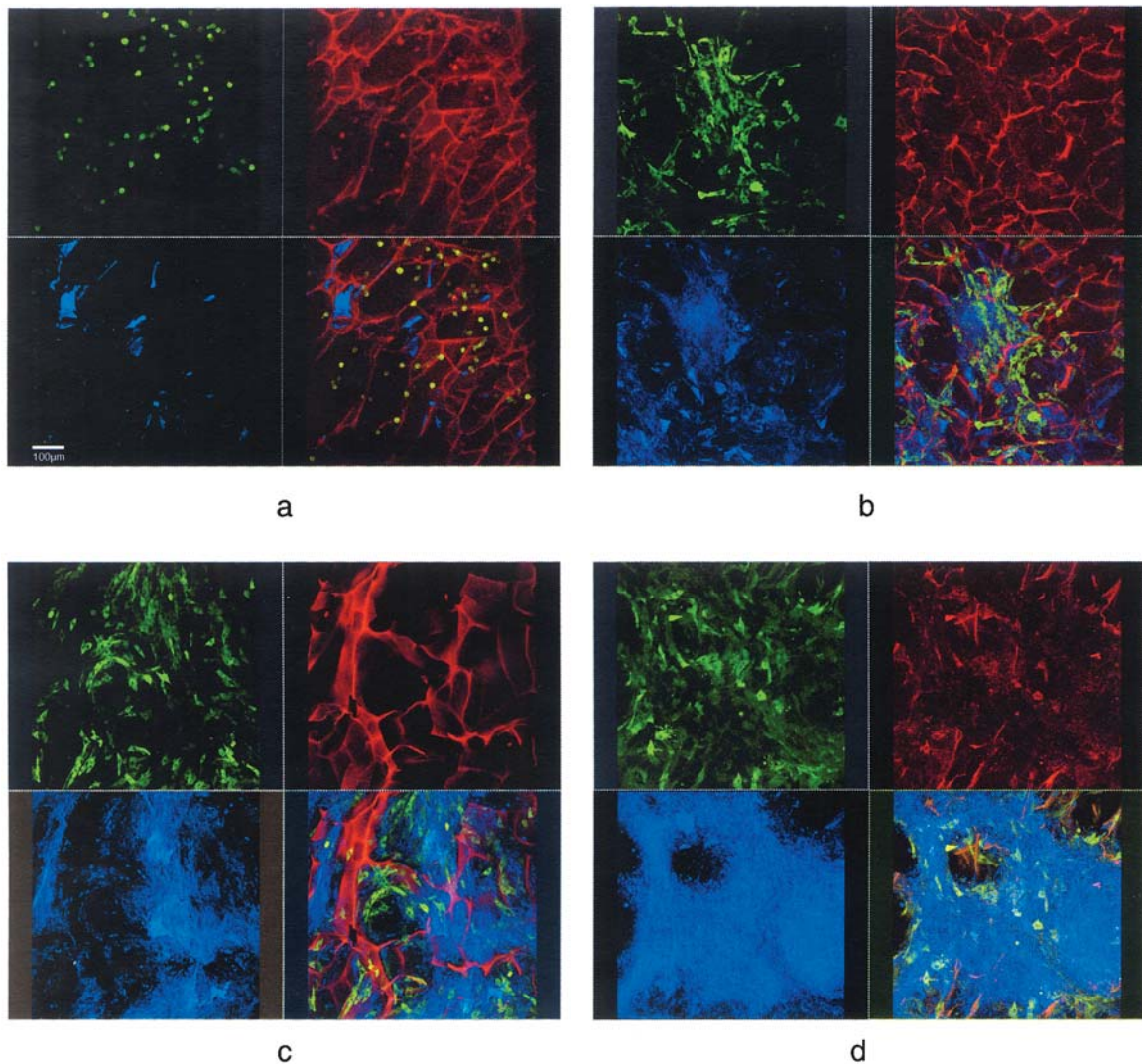


FIG. 2. Confocal microscopy of cells attaching to the 100- μm chitosan scaffold (**a–d**). x - y projections of 3-D data sets after 1 day (**a**), 3 days (**b**), 5 days (**c**), and 7 days (**d**) of culture. In the three-color images, red represents the autofluorescence signal from the chitosan scaffold, green represents the GFP–vinculin signal expressed by cells, and blue represents the reflection signal from the tissue, contributed mostly by the secreted matrices. The scale bar represents 100 μm .

the spherically shaped cells. During the next stage, with increasing amounts of matrix secretion (the blue fiber-like structures in the images), cells exhibit an elongated morphology and express increasing amounts of vinculin, suggesting greater cell–cell interactions and cell–matrix adhesion (Fig. 2b and c). Figure 2d shows the tissue in the later culture period, when various cell morphologies are found and the amount of vinculin expression by cells is decreased. At this time point, the reflected signals from the secreted matrix are intense, and the chitosan scaffold is diminished within about 150 μm of the tissue surface. This result can be explained with correlations to the corresponding OCT and histological images (Fig. 1d and i), where the tissue is found to have a thick surface layer of cells and matrices. Cells at this late stage migrate to the

surface, lose functionality, and form collections near the tissue surface. For further visualization, an ultrahigh resolution SEM micrograph (Fig. 11) shows surface morphology of the chitosan scaffold, cell morphology, and matrix secreted by the cells, illustrating the spatial relationships among the three tissue components.

Compared with conventional invasive, destructive imaging techniques such as histology and SEM, OCT and CM are nondestructive, real-time, time-lapse imaging methods that reveal similar cell and tissue characteristics such as tissue development stage, tissue architecture, cell distribution, cell morphology, and cell–matrix interaction. The elimination of specimen fixation and extensive processing reduces the possibility of structural artifacts and facilitates repeated observations within a single sam-

ple over time, and in response to various internal and external chemical and mechanical stimuli. Furthermore, there is minimal disturbance to the cell and tissue physiology of the living samples, because (1) living samples are imaged in a sterile microincubator under physiological conditions; (2) the laser power used to acquire images is low; and (3) the imaging speed is fast, requiring only a few seconds to acquire an OCT or CM image. In addition, OCT and CM can also provide complementary information about the engineered tissue. OCT is able to image deep (up to 2 mm in this study) into the highly scattering tissue, and reveal the cell distribution and tissue microarchitecture. CM is used to visualize the spatial distribution of scaffold, matrix, and cell-specific fluorescent probes near the tissue surface. Both OCT and CM can provide real 3-D image information, which conventional invasive methods cannot provide.

Structural properties of engineered tissue demonstrated by 3-D OCT

The 3-D visualization of an engineered tissue *in vitro* can be achieved by volume rendering a series of cross-sectional OCT images. By assembling sequential cross-sectional OCT images with 20- μm interval spacing, using 3-D reconstruction software (Slicer Dicer; Pixotec), we obtained 3-D structural information about the engineered tissues longitudinally over time (Fig. 3). We were able to visualize the interior of the tissue from various viewpoints with arbitrary sectioning planes at any angle and direction (Fig. 3a–c). This provides a substantial improvement over 2-D cross-sectional images, and proves to be significantly more useful than histological sections, which are confined to a single plane through the tissue block.

Because the digitized 3-D OCT images represented the full volume of the engineered tissues, we investigated both tissue porosity and cell distribution during growth. The engineered tissue clearly exhibited a porous microarchitecture, which accounts for the time-dependent cell distribution phenomena. Figure 3a–d reveals a highly porous 3-D microarchitecture, which is beneficial for

deep nutrient penetration into the tissue volume. In contrast, the sample in Fig. 3e has a thick cell–matrix layer on the surface. The 3-D reconstruction further shows that there were almost no open pores on the surface of the structure that would allow the routine diffusional exchange of nutrients and wastes. The blockage of these pathways may deprive cells deep inside the scaffold of nutrients, leading to necrosis. This deprivation may also have caused the observed cell migration to the surface. Initially, cells in the scaffolds were uniformly distributed spatially throughout the matrix, which was shown in both the histological image (Fig. 1a) and the OCT image (Fig. 1f). At longer culture times, the fibroblasts, the major matrix-secreting cells, continuously deposited matrix, thus narrowing or completely blocking the pores.

Importantly, these results demonstrate the powerful ability of OCT to aid in the interpretation of structural changes of engineered tissues, especially the complex interrelationships, in both space and time, of key structural features that can only be inferred from 2-D cross-sectional images. These results demonstrate the potential of OCT for visualizing complex 3-D microstructure and morphology in engineered tissue development. Although the chitosan scaffold-based model used in this study is a relatively homogeneous engineered tissue model, the composition of engineered tissues is becoming increasingly more heterogeneous in order to replicate *in vivo* structures and mimic physiological functions. Three-dimensional OCT imaging is likely to be advantageous for tracking the evolving morphology of heterogeneous engineered tissues over time.

Functional properties demonstrated by 3-D confocal microscopy

In addition to dynamic 3-D cell and tissue-level information, tissue engineering also requires functional assessments at both the cellular and molecular levels. Previous studies of cell–matrix or cell–cell interactions primarily used immunohistology and imaged with conventional light or confocal microscopy. This invasive methodology required the excision and fixation of sam-

FIG. 3. Three-dimensional reconstructed OCT images of engineered tissue. Reconstructed volumes were rendered with Slicer Dicer and viewed at three rotational angles. *Top*: -60° (y), 20° (z), 70° (x). *Middle*: -40° (y), -20° (z), 70° (x). *Bottom*: 0° (y), 10° (z), -50° (x). Three-dimensional volumes are reconstructed from different numbers of cross-sectional slices: 6 (a), 12 (b), and 50 (c). The engineered tissues were cultured for 3 days (a–c), 5 days (d), and 7 days (e). The scale bar represents 200 μm (1 pixel = 3.9 μm).

FIG. 4. Three-dimensional reconstructed confocal microscopy images of engineered tissue (a–c). Reconstructed images are shown with different rotational angles: (a) -120° (x), 20° (y), -15° (z); (b) -70° (x), 30° (y), -45° (z); and (c) 45° (x), 50° (y), -55° (z). To emphasize structure, the tissue network is shown in three-dimensions, where all signals have the same color (d). Cell–cell and cell–substrate interactions are shown with cross-sectional slices or volume images (e–h). The engineered tissues shown are between 3 and 5 days of culture. The scale bars shown in (a–f) all represent 100 μm . The scale bars shown in (g) and (h) represent 50 and 20 μm , respectively.

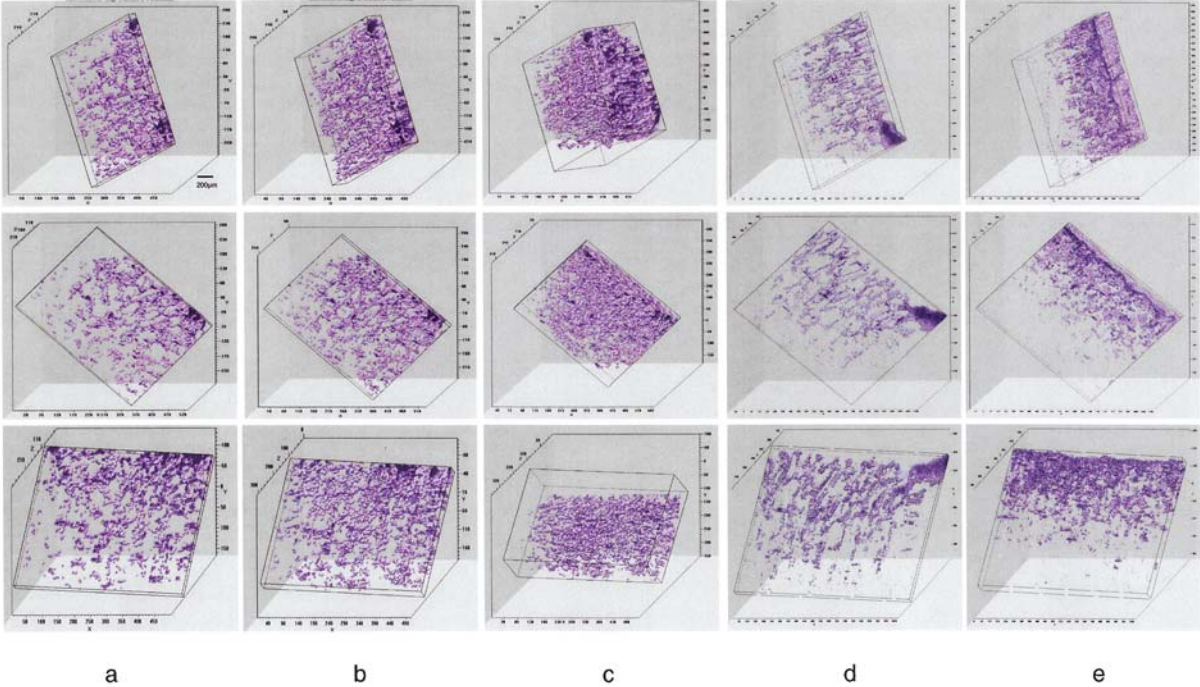


FIG. 3.

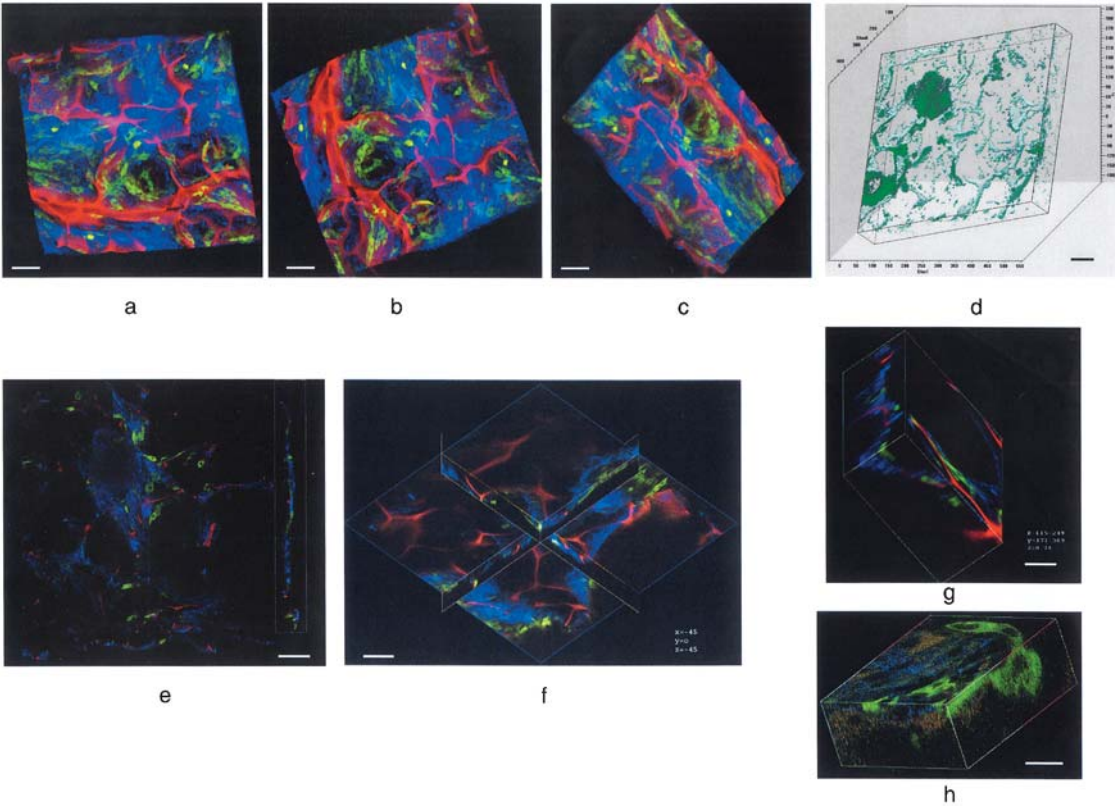


FIG. 4.

ples, and the subsequent loss of spatial information concerning sample location within a 3-D tissue.^{23,24} However, developments in optical microscopy, contrast agents, and probe engineering have made it possible to avoid the use of chemical dyes to detect transient interactions. Using transfected GFP–vinculin and a commercial fluorescence separation algorithm (Leica Microsystems), we have successfully demonstrated the use of CM to simultaneously study cell morphology, matrix secretion, and scaffold structure to obtain real-time molecular level information about cell–cell and cell–matrix interactions in 3-D engineered tissues. The dye separation algorithm was able to separate the emitted GFP fluorescence from the background chitosan scaffold autofluorescence by at least a factor of two.

Confocal microscopy was used to visualize the cell–cell and cell–substrate interaction in three dimensions (Fig. 4). Figure 4a–c shows the reconstructed images of engineered tissue at different rotational angles after 5 days of culture. Figure 4a–c shows the cell positions in three dimensions and their spatial relationship to other cells, the matrices, and the scaffolds. We expressed a GFP–vinculin fusion protein in fibroblasts to monitor cell–cell and cell–matrix interactions in engineered tissue because vinculin expression reflects the degree of cell–cell and cell–substrate adhesions. The scaffold provides physical cues for cell orientation and spreading, and pores provide space for the remodeling of tissue structures by matrix secretion. The reconstructed 3-D images (Fig. 4d) show similar tissue architecture as in the OCT images, but the imaging depth of CM is significantly less, being about 150 μm . As reported by Cukierman and others,²⁴ patterns of focal adhesions in 3-D scaffolds differ significantly from those found in 2-D cultures. Figure 4e–h shows the cell–cell and cell–substrate interactions within the tissue volume, displayed as volumetric CM data sets, and selected cross-sectional slices through these volumes. Here, the extracellular matrix, which mediates cell–substrate attachment, is always found between vinculin and the scaffold. However, the distribution of matrix material is not uniformly proportional to the vinculin density (Fig. 4e–g). This may be due to the surface topography of the scaffold and the nature by which pseudopodia from the cells become interconnected (Fig. 4h).

The GFP used in this study is a well-established gene expression marker for labeling intact cells and whole organisms. This protein has been used to successfully target and label nearly every major organelle of the cell, as well as many subcellular proteins.^{25–27} By using GFP for functional imaging of living cells, real-time information about cellular functions and responses can be obtained, such as the 3-D distribution of cell–cell and cell–matrix activity visualized in this study. Time-lapse confocal reflectance microscopy has been used for surface and volume visualization of intact extracellular matrix.^{28,29}

Without the use of fluorescent probes, this noninvasive method for observing extracellular matrix deposition in three dimensions is based on a natural source of contrast provided by absorption and scattering changes in the microscopic structure of tissue. Confirmed in our study, scattering indices from this secreted matrix increase the intensity of backreflected light and can be imaged by confocal reflectance microscopy.

Implications for tissue-engineering research

This article illustrates a new approach in the use of OCT and CM visualization techniques to reconstruct 3-D information about engineered tissue development over time. The complementary use of OCT and CM to provide microstructural and functional information within *in vitro* engineered tissue is reported. OCT can penetrate significantly deeper than CM and has a larger field of view, thus giving a general picture of the cell distribution and microarchitecture within engineered tissues. With functional sites labeled on cells, CM can use the near-surface cells as a sampling population for overall tissue function and can monitor the near-surface 3-D spatial distribution of functional markers to determine their location, functional properties, and physiological responses to the engineered tissue matrix. The complementary use of OCT and CM to assemble all the information collected from the parameters of a cell and its environment will more accurately reflect the architecture and dynamic properties of the tissue. Conventional CM approaches often provide only regional data that have been specifically tagged by fluorescent probes. Furthermore, it is feasible to integrate the optical elements of OCT with confocal and multiphoton microscopy.^{30,31} In particular, multiphoton microscopy and OCT can be performed simultaneously, using the same titanium:sapphire laser source.³¹ To integrate OCT imaging with confocal or multiphoton microscopy in the same instrument, an *en face* OCT scanning mode is used, collecting images (sections) that are parallel to the surface of the specimen. With *en face* OCT scanning, high lateral (transverse) resolution can be achieved by using high numerical aperture objectives. The use of high numerical aperture objectives, however, results in short depths of focus, requiring the additional use of focus-tracking techniques to keep the OCT coherence gating region aligned with the tight beam focus. At the same time, the penetration depth will be decreased when using high numerical aperture lenses because of their short working distances between the objective and the focal region. Despite these additional complexities, by integrating these optical imaging techniques in a single microscope, morphological and functional characteristics of engineered tissues could be imaged by OCT, concurrently with site-specific labeling and quantification of focal adhesion sites with

fluorescence-based microscopy techniques (CM, multiphoton microscopy). These capabilities are ideally suited for real-time diagnostic analysis and monitoring during growth of engineered tissue structures.

The approaches described in this article are likely to have broad impact in a wide range of applications involving engineered tissues. These can be broadly classified into therapeutic applications, where the tissue will be transplanted into a patient, and diagnostic applications, where the tissue will be used for basic science studies in cell and tissue biology, or for pharmacological testing of drug metabolism, uptake, toxicity, and pathogenicity. The process of forming tissues from cells is a highly orchestrated set of events that occur over time scales ranging from seconds to weeks, and with dimensions ranging from 1 μm to 1 cm. Current research and development has addressed these problems separately at either end of this spectrum with studies of basic biological and biophysical processes at the molecular level, or with studies of tissue morphology at discrete time points. In the studies presented here, the 3-D spatial information from engineered tissues can be obtained at size scales ranging from the molecular level, using molecule-specific probes, to the cell and tissue levels. Dynamic information representing up to four dimensions (x , y , z , and time) can be readily collected and reconstructed for purposes of visualization and quantitative analysis. The additional dimensions of 3-D space and time are likely to have a significant impact on tissue-engineering research. Future work will focus on improving spatial and temporal resolutions and the further integration of multimodality optical imaging techniques.

The OCT imaging modality holds promise for applications in cell and tissue biology, tissue engineering, and drug discovery. This nondestructive method for assessing tissue development is likely to significantly enhance our ability to formulate and direct a strategy for identifying and implementing optimal culture conditions that support tissue development *in vitro*. With deep imaging penetration depth and high spatial and temporal resolution in three dimensions, OCT will be a powerful tool for gaining new insights into cell dynamics in real time, for elucidating complex biological interactions, and for directing new engineering approaches toward functional, biomimetic, and mature engineered tissues.

ACKNOWLEDGMENTS

The authors thank Dr. Benjamin Geiger (Weizmann Institute of Science, Israel) for providing the GFP-vinculin plasmid for this work. The authors also thank Drs. Dan Marks and Amy Oldenburg for their efforts in developing and maintaining the OCT imaging system. This work was supported in part by the National Institutes of

Health (NIBIB, 1 R01 EB00108-1, S.A.B.), the University of Illinois Critical Research Initiative (S.A.B.), the National Institutes of Health (GMS, 1 R01 51338, D.E.L.), the National Aeronautics and Space Administration (NASA, NAG8-1922, R.J. and A.S.), and the University of Illinois Intercampus Research Initiative in Biotechnology (A.S.).

REFERENCES

1. Langer, R., and Vacanti, J.P. Tissue engineering. *Science* **260**, 920, 1993.
2. Friedrich, M.J. Studying cancer in 3 dimensions. *JAMA* **290**, 1977, 2003.
3. Stephens, D.J., and Allan, V.J. Light microscopy techniques for live cell imaging. *Science* **300**, 82, 2003.
4. Breuls, R.G.M., Mol, A., Pettersson, R., Oomens, C.W.J., Baaijens, F.P.T., and Bouten, C.V.C. Monitoring local cell viability in engineered tissues: A fast, quantitative, and nondestructive approach. *Tissue Eng.* **9**, 269, 2003.
5. Gareau, D.S., Bargo, P.R., Horton, W.A., and Jacques, S.L. Confocal fluorescence spectroscopy of subcutaneous cartilage expressing green fluorescent protein versus cutaneous collagen autofluorescence. *J. Biomed. Opt.* **9**, 254, 2004.
6. Clark, A.L., Gillenwater, A.M., Collier, T.G., Alizadeh-Naderi, R., El-Naggar, A.K., and Richards-Kortum, R.R. Confocal microscopy for real-time detection of oral cavity neoplasia. *Clin. Cancer Res.* **9**, 4714, 2003.
7. Sung, K.B., Liang, C., Descour, M., Collier, T., Follen, M., and Richards-Kortum, R. Fiber-optic confocal reflectance microscope with miniature objective for *in vivo* imaging of human tissues. *IEEE Trans. Biomed. Eng.* **49**, 1168, 2002.
8. Tachihara, R., Choi, C., Langley, R.G., Anderson, R.R., and Gonzalez, S. *In vivo* confocal imaging of pigmented eccrine poroma. *Dermatology* **204**, 185, 2002.
9. Masters, B.R., So, P.T., and Gratton, E. Multiphoton excitation microscopy of *in vivo* human skin: Functional and morphological optical biopsy based on three-dimensional imaging, lifetime measurements and fluorescence spectroscopy. *Ann. N.Y. Acad. Sci.* **838**, 58, 1998.
10. So, P.T., Dong, C.Y., Masters, B.R., and Berland, K.M. Two-photon excitation fluorescence microscopy. *Annu. Rev. Biomed. Eng.* **2**, 399, 2000.
11. Constantinidis, I., Stabler, C.L., Long, R., Jr., and Sambanis, A. Noninvasive monitoring of a retrievable bioartificial pancreas *in vivo*. *Ann. N.Y. Acad. Sci.* **961**, 298, 2002.
12. Lin, A.S.P., Barrows, T.H., Cartmella, S.H., and Guldberg, R.E. Microarchitectural and mechanical characterization of oriented porous polymer scaffolds. *Biomaterials* **24**, 481, 2003.
13. Huang, D., Swanson, E.A., Lin, C.P., Schuman, J.S., Stinson, W.G., Chang, W., Hee, M.R., Flotte, T., Gregory, K., and Puliavito, C.A. Optical coherence tomography. *Science* **254**, 1178, 1991.
14. Bouma, B.E., and Tearney, G.J. *Handbook of Optical Coherence Tomography*. New York: Marcel Dekker, 2001.
15. Schmitt, J.M. Optical coherence tomography (OCT): A review. *IEEE J. Select. Topics. Quant. Electr.* **5**, 1205, 1999.

16. Fujimoto, J.G. Optical coherence tomography for ultrahigh resolution *in vivo* imaging. *Nat. Biotechnol.* **21**, 1361, 2003.
17. Boppart, S.A., Boumal, B.E., Pitris, C., Southern, J.F., Brezinski, M.E., and Fujimoto, J.G. *In vivo* cellular optical coherence tomography imaging. *Nat. Med.* **4**, 861, 1998.
18. Podoleanu, A.G., Rogers, J.A., Jackson, D.A., and Dunne, S. Three dimensional OCT images from retina and skin. *Opt. Exp.* **7**, 292, 2000.
19. Boppart, S.A., Brezinski, M.E., Bouma, B.E., Tearney, G.J., and Fujimoto, J.G. Investigation of developing embryonic morphology using optical coherence tomography. *Dev. Biol.* **177**, 54, 1996.
20. Boppart, S.A., Tearney, G.J., Bouma, B.E., Southern, J.F., Brezinski, M.E., and Fujimoto, J.G. Noninvasive assessment of the developing *Xenopus* cardiovascular system using optical coherence tomography. *Proc. Natl. Acad. Sci. U.S.A.* **94**, 4256, 1997.
21. Xu, X., Wang, R.K., and El Haj, A. Investigation of changes in optical attenuation of bone and neuronal cells in organ culture or three-dimensional constructs *in vitro* with optical coherence tomography: Relevance to cytochrome oxidase monitoring. *Eur. Biophys. J.* **32**, 355, 2003.
22. Mason, C., Markusen, J.F., Town, M.A., Dunnill, P., and Wang, R.K. The potential of optical coherence tomography in the engineering of living tissue. *Phys. Med. Biol.* **49**, 1097, 2004.
23. Zajackowski, M.B., Cukierman, E., Galbraith, C.G., and Yamada, K.M. Cell-matrix adhesions on poly(vinyl alcohol) hydrogels. *Tissue Eng.* **9**, 525, 2003.
24. Cukierman, E., Pankov, R., Stevens, D.R., and Yamada, K.M. Taking cell-matrix adhesions to the third dimension. *Science* **294**, 1708, 2001.
25. Balaban, N.Q., Schwarz, U.S., Riveline, D., Goichberg, P., Tzur, G., Sabanay, I., Mahalu, D., Safran, S., Bershadsky, A., Addad, L., and Geiger, B. Force and focal adhesion assembly: A close relationship studied using elastic micropatterned substrates. *Nat. Cell Biol.* **3**, 466, 2001.
26. Tsien, R.Y. The green fluorescent protein. *Annu. Rev. Biochem.* **67**, 509, 1998.
27. Lippincott-Schwartz, J., and Patterson, G.H. Development and use of fluorescent protein markers in living cells. *Science* **300**, 87, 2003.
28. Voytik-Harbin, S.L., Rajwa, B., and Robinson, J.P. Three-dimensional imaging of extracellular matrix and extracellular matrix-cell interactions. *Methods Cell Biol.* **63**, 583, 2001.
29. Brightman, A.O., Rajwa, B.P., Sturgis, J.E., McCallister, M.E., Robinson, J.P., and Voytik-Harbin, S.L. Time-lapse confocal reflection microscopy of collagen fibrillogenesis and extracellular matrix assembly *in vitro*. *Biopolymers* **54**, 222, 2000.
30. Dunkers, J.P., Cicerone, M.T., and Washburn, N.R. Co-linear optical coherence and confocal fluorescence microscopies for tissue engineering. *Opt. Exp.* **11**, 3074, 2003.
31. Beaurepaire, E., Moreaux, L., Amblard, F., and Mertz, J. Combined scanning optical coherence and two-photon-excited fluorescence microscopy. *Opt. Lett.* **24**, 969, 1999.

Address reprint requests to:
Stephen A. Boppart, M.D., Ph.D.
Beckman Institute for Advanced
Science and Technology
University of Illinois at Urbana-Champaign
Urbana, IL 61801

E-mail: boppart@uiuc.edu